Influence of boundary geometry in domain wall propagation in magnetic films with asymmetric holes: micromagnetic calculations.

A Alija[1]**, I Sobrado**[1]**, G Rodríguez-Rodríguez**[1]**, M Vélez**[1]**, J M Alameda**[1] **and J M R Parrondo**[2] **and J I Martín**[1]

[1]Dpto. Física. Fac. Ciencias. Universidad de Oviedo - CINN. 33007, Oviedo - Spain
[2]Dpto. Física Atómica, Molecular y Nuclear and GISD. Universidad Complutense de Madrid. 28040, Madrid - Spain

E-mail: `a.alija@cinn.es`

Abstract.
　Micromagnetic simulations have been performed in uniaxial magnetic films with 2D array of asymmetric arrow shape holes. In order to understand the asymmetric pinning potential created by the holes, different boundary geometries conditions are used on the simulations. The depinning fields for forward and backward domain wall propagation have been calculated by the analysis of the energy landscapes as a function of the domain wall position. Domain wall depinning occurs preferentially at the free ends of the domain wall at the film boundaries. We have found that the domain wall propagation is different at the top/bottom boundaries of the simulated film which can be understood in terms of the magnetostatic energy and the chirality of the domain wall.

1. Introduction

Domain wall (DW) propagation in thin films has been widely studied because of its relevance in determining magnetization reversal processes as the basis of a number of magnetic devices [1]. More recently, DW motion has been studied in magnetic circuits or magnetic conduits [2]. Thanks to the development of modern lithographic techniques for the fabrication of magnetic nanostructures [3], DW motion in nanowires has been used to develop different kinds of DW logic and memory devices [4, 5]. Controlled defects such as non-magnetic holes in thin films [6] or notches in nanowires [7, 8] have been used to provide effective pinning centres to control DW motion. A case of particular significance is the development of devices that can control the sense of propagation of DW within the system, i. e. the so-called 'magnetic ratchets'. Recently, it has been shown that, for a DW moving in a thin film with a periodic array of asymmetric holes, the preferred sense of propagation depends on whether a flat or a kinked wall is moving [10]. The interplay between these two ratchet effects of opposite sign provides a memory effect that could be useful for device applications. Experimentally, DW motion has been previously studied in nano-structured amorphous CoSi soft magnetic films deposited on Si substrates [10]. A large 2D array of asymmetric non magnetic holes has been patterned on these films by using *e*-beam lithography and dry etching techniques [9]. From the theoretical point of view, the study of

the motion of domain walls has been done in the framework of a ϕ^4 model [10] with periodic boundary conditions, however actual experiments are performed on finite size patterned films.

In this work, the pinning potential created by the asymmetric holes will be analysed by micromagnetic simulations using OOMMF code [11] depending on boundary geometry of the finite magnetic film.

2. Micromagnetic Calculations Details

Micromagnetic simulations have been performed with the OOMMF code. Thus, several arrays of empty arrow shape holes have been defined in rectangular thin film elements (so as to simulate the patterned continuous film) with material parameters corresponding approximately with those of the CoSi alloy: $M_s = 2 \cdot 10^5 A \cdot m^{-1}$, $A = 3 \cdot 10^{-11} J \cdot m^{-1}$ and uniaxial anisotropy $K = 1000 J \cdot m^{-3}$ with the easy axis oriented in the y direction [12]. Typical mesh sizes 15 nm up to 35 nm have been used, smaller than both the material exchange length, $\delta_{\text{ex}} = (2A/\mu_0 M_S^2)^{1/2} = 35$ nm, and the Bloch parameter $\delta_0 = (A/K)^{1/2} = 170$ nm [13]. The simulated structures are embedded in a rectangular film 28×28 μm^2 and 35 nm thick. Elements are asymmetric arrows 4 μm wide $\times$ 4 μm height set in a vertical line where the distance between two of these elements is between $d = 3$–4 μm. The direction in which the arrow tip is pointing out (forward direction) is aligned perpendicular to the uniaxial anisotropy easy axis.

3. Results and discussion

Figure 1(a) shows a micromagnetic simulation where a Néel type domain wall was placed in the middle of the film dividing two domains magnetized in opposite directions along the easy axis. The inter-hole distance is set to d = 4 μm. The size of the holes is $D = 4$ μm too. Afterwards by applying a constant magnetic field $H = 2$ mT, parallel to the magnetic easy axis, the DW is forced to move forward towards an array of arrow shape holes until the DW reaches the array of holes and becomes pinned on the holes. Figure 1(b) shows a DW that is still pinned on the holes, but that has proceeded a small distance forward upon the pressure of the applied field. The free ends of the DW at the top/bottom film boundaries propagate more easily than DW segments that are pinned in between two arrow holes. It must be noted that the DW exhibits different displacements at the top and bottom boundaries of the film. The bottom segment of the DW has moved further than the upper segment of it along the boundaries of the film.

In figure 1(c) the situation is rather similar to the case of figure 1(a) but now, a half defect is placed on the boundaries of the film in order to pin more efficiently these top/bottom DW free ends. The inter-hole distance is now set to $d = 3$ μm but the hole size is kept equal $D = 4$ μm. In figure 1(d) it can be seen that, these half defects pin more efficiently the top DW end but the bottom end of the DW keeps moving further along the bottom boundary. It even exceeds the pinning potential created by the half defect, so that the DW segment develops a semi kink.

Figure 1(e) represents the total energy minus the energy term due to the external magnetic field applied (the Zeeman energy contribution) *versus* normalized (absolute value) magnetization along the easy axis of the magnetic film. This representation has been previously used in [14] to determine several relevant aspects of the DW behavior across the asymmetric array. These graphs provide insight into the characteristic depinning landscape created by the arrow holes such as backward/forward pinning fields (B_B and B_F). First feature that we can easily extract from this figure is that the pinning energy potential reproduces the asymmetric shape of the arrow holes because there are two well defined different slopes. Following figure 1(e) from left to right we can travel along pinning energy as a function of DW average position. For instance, the minimum in the potential energy profile (e) corresponds to figure 1(a) or (c) depending on which curve we are focusing (blue or black respectively).

From the slopes of the energy curves [14] we have calculated B_B (abrupt slope) or B_F (gradual slope). For blue curve, (red dotted line) $B_B = 2.67$ mT whereas for the black curve B_B
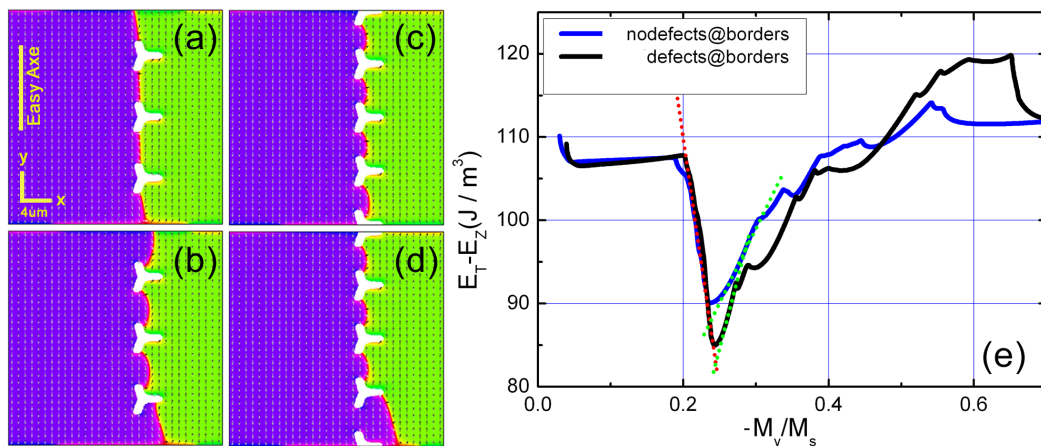
Figure 1. (a–d) Micromagnetic simulation of a Néel DW pinned in an array of 4 μm arrow shape holes under a constant field of 2 mT: (a) and (c) DW pinned at minimum energy. (b) and (d) DW just before depinning from the lowest arrow hole. (e) Energy profile corresponding to simulations (a-d). In this graph total energy minus Zeeman energy term is plotted as a function of M_y/M_s (approximately proportional to average wall position). Blue curve corresponds to a simulations (a–b). Black curve corresponds to simulations (c–d) with half defect placed in both boundaries of the film. Note that as the wall proceeds in the forward direction the magnetization becomes more negative. Dotted lines are linear fits.

is 3.34 mT. The same calculation extracted both from the gradual slope gives $B_F = 0.97$ mT (blue) and $B_F = 1.7$ mT (black). From the data it is clear that adding the half defects at the boundaries and decreasing inter-hole distances, both forward and backward fields become larger as could be expected.

But what it is not so straightforward is the fact that the DW moves more easily along the bottom boundary in both simulations. From the images it is clear that the DW segments at the center of the film are pinned more efficiently than the segments at the top and bottom borders. From the point of view of DW elastic energy, figures 1(c) and (d) show the same geometry of the pinning holes but the pinning efficiency for the bottom DW segment appears still weaker. However, in order to further understand the influence (in depinning fields) on both, top and bottom boundaries of the film, we have to take into account not only the elastic energy but also the magnetostatic energy and the chirality of the DW.

Figure 2 shows a map of the divergences of the magnetization for the simulations of figures 1(b) and (d). These maps give information about the distribution of the magnetic charges and thus of the magnetostatic energy. Focusing on a DW segment pinned in between two arrow holes, it can be seen that the charge distribution changes along the DW with more positive/negative charges at the top/bottom ends. (see boxes in figure 2(b)). Thus there must be a significant magnetostatic interaction between two DW ends across an arrow hole. This implies a higher pinning efficiency of the central defects in comparison with the half defects placed at the boundaries of the film (as seen in figure 1(d)).

Concerning the easier propagation of the DW along the bottom boundary than at the top boundary of the film, it can be attributed to the chirality of the Néel DW (fixed by the initial conditions). Chirality of the DW determines which of the two free endings of the DW is kept pinned and which is depinned on the half arrow ending defect in a similar way as reported by D. Petit, *et al.* [15] in experiments of domain wall propagation under pinning potential landscapes created by constrictions and protrusions in permalloy nanowires.
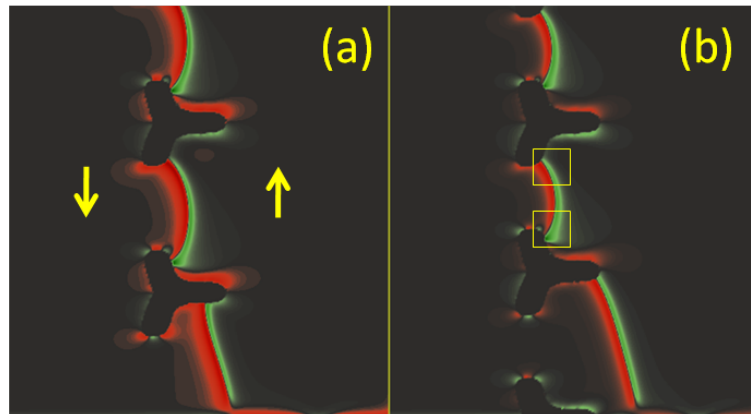
Figure 2. Divergence map of the magnetization for (a) simulation with no defects on the boundary and (b) simulation with half defect on the boundary of the film. Arrows indicate the direction of the magnetization.

4. Conclusions

To conclude, we have performed micromagnetic simulations to study the Néel domain wall motion on a ferromagnetic film patterned with a 2D array of asymmetric arrow shape holes. The pinning efficiency of the asymmetric arrow shape holes depends on the distance between the holes. The pinning strength on the domain wall is weaker at the boundaries of the film than at the center. When a half defect is placed at top/bottom film boundaries the domain wall is pinned more efficiently, however the propagation of the domain wall remains still easier along the bottom border of the film than along the top border. Magnetostatic interactions and domain wall chirality appears as the key factors to explain the different pinning efficiencies observed along the domain wall.

References

[1] G. Prinz, *J. Magn. Magn. Mater.* **200** 57 (1999)
[2] E.R. Lewis, *et al. Phys. Rev. Lett.* **102**, 057209 (2009)
[3] J. I. Martin, *et al J. Magn. Magn. Mater.* **256** 449 (2003)
[4] D. A. Allwood, *et al. Science* **296** 2003 (2002)
[5] S. Parkin, *et al. Science* **320** 5873 190 (2008)
[6] A. Perez-Junquera, *et al J. Appl. Phys.* **99** 033902 (2006)
[7] T. Ono, *et al. Appl. Phys. Lett.* **72** 1116 (1998)
[8] S. Savelev, *et al. Phys. Rev.* B **74** 024404 (2006)
[9] A. Perez-Junquera, *et al. Nanotechnology* **15** S131, (2004)
[10] A. Perez-Junquera, *et al. Phys. Rev. Lett.* **100** 037203 (2008)
[11] OOMMF User's Guide, Version 1.0 M.J. Donahue and D.G. Porter *Interagency Report NISTIR* **6376**, NIST, Gaithersburg, MD (Sept 1999)
[12] M. Velez , *et al. Eur. Phys. Lett.* **41** 517 (2004)
[13] A. Hubert and R. Shafer. Magnetic Domains. *The analysis of magnetic microstructures.* Springer-Verlag, New York (1998).
[14] A. Alija, *et al. J. Phys.* D: *Appl. Phys.* **42** (2009) 045001
[15] D. Petit, *et al. J. Appl. Phys.* **103** 114307 (2008)